International Conference on Mathematics and Computational Methods Applied to Nuclear Science and Engineering (M&C 2011)
Rio de Janeiro, RJ, Brazil, May 8-12, 2011, on CD-ROM, Latin American Section (LAS) / American Nuclear Society (ANS)
ISBN 978-85-63688-00-2

A PIECEWISE BI-LINEAR DISCONTINUOUS FINITE ELEMENT SPATIAL DISCRETIZATION OF THE Sn TRANSPORT EQUATION

Teresa S. Bailey
Lawrence Livermore National Laboratory
P.O. Box 808, L-095
Livermore, CA 94551
bailey42@llnl.gov

James S. Warsa and Jae H. Chang
Los Alamos National Laboratory
P.O. Box 1663, MS D409
Los Alamos, NM 87544
warsa@lanl.gov; jhchang@lanl.gov

Marvin L. Adams
Texas A&M University
Department of Nuclear Engineering
College Station, TX 77843-3133
mladams@tamu.edu

ABSTRACT

We present a new spatial discretization of the discrete-ordinates transport equation in two-dimensional Cartesian (X-Y) geometry for arbitrary polygonal meshes. The discretization is a discontinuous finite element method (DFEM) that utilizes piecewise bi-linear (PWBL) basis functions, which are formally introduced in this paper. We also present a series of numerical results on quadrilateral and polygonal grids and compare these results to a variety of other spatial discretizations that have been shown to be successful on these grid types. Finally, we note that the properties of the PWBL basis functions are such that the leading-order piecewise bi-linear discontinuous finite element (PWBLD) solution will satisfy a reasonably accurate diffusion discretization in the thick diffusion limit, making the PWBLD method a viable candidate for many different classes of transport problems.

Key Words: DFEM, Polygonal Grids, thick diffusion limit, deterministic transport

1. INTRODUCTION

Recently, spatial discretizations for the Sn transport equation have been developed for arbitrary polygonal grids with straight edges in both R-Z and X-Y geometry [1, 2, 3, 4, 5, 6, 7]. Spatial discretizations that are successful on these grid types allow for more flexible transport solutions in radiative transfer systems as well as on AMR grids. In this paper, we present a new method for polygonal grids. This method is a standard Galerkin DFEM that utilizes Piecewise Bi-linear (PWBL) basis functions, giving rise to the Piecewise Bi-linear Discontinuous Finite Element method (PWBLD). These functions are developed similarly to the Piecewise Linear (PWL)

basis functions [1, 2, 7], but are fundamentally different in that they are based on a certain quadrilateral sub-division on convex polygons and reduce to bi-linear functions on quadrilaterals.

We first define the Galerkin DFEM discretization applied to the X-Y Sn equation. We then define the PWBL basis functions and show how these functions are introduced into the standard DFEM discretization. We show equivalence to BLD on quadrilateral grids using numerical test problems. We then present results on polygonal grids that demonstrate the method can be used to compute reasonably accurate interior solutions in the thick diffusion limit in presence of unresolved boundary layers. A desired characteristic of the previously developed methods for polygonal grids is that the methods produce good numerical behavior in the thick diffusion limit. Although we do not provide details of the asymptotic analysis that predicts and explains this good numerical behavior, we note that the PWBLD method possesses the properties shown in reference [8] to be necessary and sufficient for accurate DFEM solutions in the thick diffusion limit.

2. DERIVATION OF THE PWBLD METHOD IN X-Y GEOMETRY

We start describing our new method with a brief derivation of a general DFEM discretization of the Sn transport equations in X-Y geometry. We complete the description of the method by defining the PWBL basis functions, with an emphasis on the similarities and differences between PWBL and PWL functions, and thus the PWBLD and PWLD methods.

2.1 General DFEM Discretization of the Sn Transport Equation

The time-independent, monoenergetic Sn transport equation in X-Y geometry with isotropic scattering is

$$\mu_m \frac{\partial}{\partial x}\psi_m(x,y) + \eta_m \frac{\partial}{\partial y}\psi_m(x,y) + \sigma\psi_m(x,y) = \frac{\sigma_s}{4\pi}\phi(x,y) + \frac{1}{4\pi}S(x,y), \quad (1)$$

where ψ is the unknown angular intensity, σ is the macroscopic total cross section, σ_s is the macroscopic scattering cross section, $\mu = \vec{e}_x \bullet \vec{\Omega}$ = x component of particle direction, $\eta = \vec{e}_y \bullet \vec{\Omega}$ = y component of particle direction, ϕ is the scalar flux, and S is a fixed source. The m subscript indicates the index of an element in the quadrature set used for the discrete-ordinates approximation [9].

The application of a discontinuous finite element method to the angularly discretized equations is straightforward and described in detail in multiple references [1, 2, 4, 6, 7, 10, 11]. A few simple steps are required to derive the DFEM spatial discretization.

1. Divide the spatial domain into domain-filling, non-overlapping, homogeneous cells.
2. Multiply the angularly discretized equations by a weight function and integrate over a spatial cell.
3. Apply Gauss's Divergence Theorem to the integrals of the gradient term, resulting in a surface integral and a volume integral. Allow the surface intensity to differ from the cell-interior intensity evaluated at the surface.
4. Expand spatially dependent fluxes and sources in terms of a set of basis functions, u_j:

$$\psi_m(x,y)=\sum_{j=1}^{J}\psi_{m,j}u_j(x,y)$$
$$\phi(x,y)=\sum_{j=1}^{J}\phi_j u_j(x,y) \tag{2}$$
$$S(x,y)=\sum_{j=1}^{J}S_j u_j(x,y)$$

5. Define each surface intensity to be the intensity from the upstream cell or boundary condition.

This procedure produces a single-cell matrix that determines the unknowns in each cell in terms of its source and its incident intensities (from upstream cells or boundary conditions). The size of this matrix is *JxJ* where *J* is the number of basis functions used to approximate the flux in the cell. The i^{th} row of a single-cell matrix is given by:

$$\oint_{\partial A_{cell}} ds v_i \vec{n}\bullet\vec{\Omega}_m\tilde{\psi}_m(x,y)-\int_{A_{cell}} dA\left(\sum_{j=1}^{J}\psi_{m,j}u_j(x,y)\right)\vec{\Omega}_m\bullet\vec{\nabla}v_i$$
$$+\int_{A_{cell}} dA v_i\sigma\left(\sum_{j=1}^{J}\psi_{m,j}u_j(x,y)\right)=\frac{1}{4\pi}\int_{A_{cell}} dA v_i\left(\sigma_s\sum_{j=1}^{J}\phi_j u_j(x,y)+\sum_{j=1}^{J}S_j u_j(x,y)\right), \tag{3}$$

where $\psi_{m,j}$ is the *j*th angular-flux unknown inside the cell, $\tilde{\psi}_m(x,y)$ is the angular flux on the cell surface, ϕ_j is the *j*th scalar-flux coefficient inside the cell, S_j is the source coefficient if we interpolate the source with the basis functions, v_i is the i^{th} weight function, and u_j is the j^{th} basis function within the cell. We have assumed that the cross sections are constant inside a spatial cell. We also note that Eq. (3) is typically solved using an iterative method where the scalar flux is determined from the previous iteration.

We use upwinding to determine the angular flux on the surface of the cell.

$$\tilde{\psi}_m(x,y)=\begin{cases}\sum_{j=1}^{J}\psi_{m,j}u_j(x,y)\ if\ \ \vec{n}\bullet\vec{\Omega}_m>0,\\ \psi_{m,upwind}(x,y)\ if\ \ \vec{n}\bullet\vec{\Omega}_m<0,\end{cases} \tag{4}$$

where the upwind angular flux is the DFEM expansion from the upwind cell for problem-interior surfaces and is the incident flux specified by the boundary condition for surfaces on the problem boundary. For the remainder of this paper we assume a Galerkin DFEM, which means that the i^{th} weight function is the same as the i^{th} basis function. Eqs. (3) - (4) are general, containing no assumptions about the shape of the cells.

2.2 The PWBL Basis Functions

The PWBL basis functions are derived similarly to the derivation of the PWL basis functions [1, 2, 7]. To build these "piecewise" functions, we divide each polygonal cell into non-overlapping subcell volumes. For PWL these subcell volumes are "sides". In 2D a side is a triangle defined by a cell center point and two adjacent vertices. For the PWBL basis functions, the subcell volume is a "corner". A 2D corner is defined as the quadrilateral created by cell center, a vertex, and the midpoints of the edges adjacent to that vertex. Corners and sides are shown in Figure 1, using a hexagonal cell as an example.

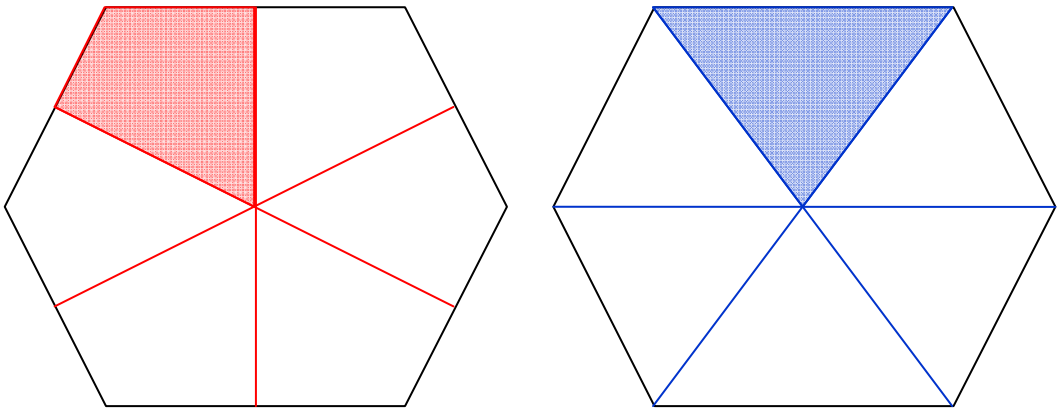

Figure 1: The shaded regions represent subcell volumes used to create Piecewise basis functions. On the left are corners for PWBL functions, on the right are sides for PWL functions defined on a hexagonal cell.

The well-known standard bi-linear functions can be mapped to each of the quadrilateral corners in the cell, and the well-known standard linear functions can be mapped to the triangular sides in the cell. A linear combination of these functions is used to form N basis functions in the cell, where N is the number of vertices in the cell. (For the cells in Figure 1, this N=6.) The PWBL basis function centered at the jth vertex can be written as

$$u_j(x,y) = b_j(x,y) + \sum_{\substack{e=edge \\ touching\ j}} \Gamma_{e,j} b_e(x,y) + \beta_j b_c(x,y), \tag{5}$$

where the functions $b(x,y)$ are standard bi-linear functions mapped to the corners. The support point for $b_j(x,y)$ is the j^{th} vertex, the support point for $b_e(x,y)$ is a cell-edge midpoint, and the support point for b_c is the cell center. The β_j and $\Gamma_{e,j}$ values are weighting parameter for the $b_c(x,y)$ and $b_e(x,y)$ contributions to each basis function, and are defined such that

$$\begin{aligned} \sum_{\substack{j=corner \\ in\ edge\ e}} \Gamma_{e,j} &= 1 \\ \sum_{j=corner} \beta_j &= 1 \end{aligned} \quad . \tag{6}$$

All calculations presented in this paper use values of

$$\begin{aligned} \beta_j &= \frac{1}{N} \\ \Gamma_{e,j} &= \frac{1}{2}, \end{aligned} \tag{7}$$

where N is the number of corners in the cell. A result of these definitions is

$$\begin{aligned} \vec{r}_c &\equiv \text{ cell midpoint } = \sum_{i=1}^{N} \beta_i \vec{r}_i = \frac{1}{N} \sum_{i=1}^{N} \vec{r}_i \\ \vec{r}_e &\equiv \text{ edge midpoint } = \sum_{\substack{i=corner \\ touching\ edge\ e}}^{2} \Gamma_{e,i} \vec{r}_i = \frac{1}{2} \sum_{\substack{i=corner \\ touching\ edge\ e}}^{2} \vec{r}_i \,, \end{aligned} \tag{8}$$

The equation defining the PWL basis function is

$$u_i(x,y) = t_i(x,y) + \beta_i t_c(x,y), \tag{9}$$

where the functions $t(x,y)$ are standard linear functions on triangles. The support point for $t_i(x,y)$ is the i^{th} vertex and the support point for $t_c(x,y)$ is the cell center. The β_i value is a weighting parameter for the $t_c(x,y)$ contributions, and is defined such that

$$\vec{r}_c \equiv \text{ cell midpoint } = \sum_{i=1}^{N} \beta_i \vec{r}_i \,. \tag{10}$$

The simplest choice of the weighting parameter, and the choice commonly used in practice, is

$$\beta_i = \frac{1}{N}, \tag{11}$$

When the PWBL basis functions are used in Eq. (3) they are easily integrated by dividing the integrals into sums of integrals over corners, causing the integrals in these equations to become

$$\begin{aligned} \oint_{\partial A_{cell}} ds &\longrightarrow \sum_{\substack{c=corners \\ \in cell}} \sum_{\substack{e_c=edges \\ \in corner}} \int_{e_c} ds \\ \int_{A_{cell}} dA &\longrightarrow \sum_{\substack{c=corners \\ \in cell}} \int_{c} dA \end{aligned} \tag{12}$$

As noted in previous work [7], the integrals for PWLD in Eq. (3) are divided into sums of integrals over sides. Both sets of basis functions are continuous within a cell, but their derivatives are discontinuous.

2.3 Differences between PWBLD and PWLD

While the PWBLD and the PWLD methods are closely related, there are important differences between the two methods. The first difference between PWLD and PWBLD is that PWLD is identical to the linear discontinuous finite element method on triangular grids, while PWBLD is algebraically equivalent to the bi-linear discontinuous finite element method on quadrilateral grids. This distinction is important because it implies that the PWBLD method offers inherently more curvature in the solution approximation as compared to PWLD when these methods are extended to polygonal grids.

The second difference between PWLD and PWBLD is the computational expense in construction of a linear system for a mesh cell. The PWBLD basis functions are significantly more complex, involving two interpolating parameters instead of one and involving an isoparametric mapping for each corner. However, both single cell linear systems are dense, JxJ matrices, where J is the number of vertices in the cell. As a result, we anticipate that if we optimize the construction of the matrix, PWBLD will be only slightly more computationally expensive than PWLD.

A third major difference between PWLD and PWBLD is the potential for extension to 3D geometry. A 3D PWLD discretization has already been developed, where tetrahedral subcell volumes are used to subdivide arbitrary polyhedral cells. The tetrahedral volumes are created using a support vertex, an adjacent vertex, the face center point for the face containing the two vertices, and a cell center point. This discretization has been thoroughly tested and shown to have the thick diffusion limit [10]. The 3D corollary for PWBLD is to subdivide a polyhedral cell into hexahedral subcell volumes. This subdivision is possible for polyhedra where each vertex in the cell is connected to 3 edges. However, if a vertex in the 3D cell is connected to more than three edges, subdividing the cell into hexahedra becomes much more complex. An example cell shape where this occurs is a square-based pyramid. The top vertex in the pyramid is connected to 4 edges. We do not believe it is impossible to extend PWBLD to 3D polyhedral cells, but a consistent subdivision of all straight-edged polyhedral cell types is currently unknown.

Finally, we have not provided here the asymptotic analysis to mathematically demonstrate that PWBLD will generate good solutions in the thick diffusion limit. However, we note that the PWBLD method meets all of the requirements shown by Adams [8] to be necessary and sufficient for accuracy in this limit. The surface integrals in the PWBLD method are identical to those in the PWLD method. As a result, Adams' surface matching property is retained. Furthermore, because we can define a PWBL basis function supported at each vertex in a polygonal cell, the PWBLD method meets Adams' full resolution requirement. It is clear from the general-DFEM analysis in [8] that for a thick diffusive problem with spatially continuous incident partial currents, the leading-order PWBLD solution will satisfy a PWBL continuous diffusion discretization with one support point (and thus one unknown) per vertex. An analysis similar to that in [10] shows that this is a reasonably accurate discretization. We remark that the

PWBLD method can employ “lumped” collision and/or surface matrices, as can other DFEMs that employ cardinal basis functions [2, 7, 12, 13]. For the sake of brevity, we do not show the lumped equations here.

3. NUMERICAL TEST PROBLEMS

We have implemented the PWBLD discretization for the XY transport equation in Capsaicin, a transport code being developed at Los Alamos National Laboratory. To test the effectiveness of the method, we used a test problem developed by Morel and Warsa [13]. This problem is a 1-D slab problem solved in 2-D with appropriate reflective boundary conditions on two of the mesh boundaries. The problem has a rectangular domain of $x \in [0, 0.25]$ and $y \in [0, 1.0]$ and $N/4 \times N$ meshes, where N is the number of mesh cells along the y axis. There is a constant isotropic distributed source, $\sigma_t = 2^{13}\, cm^{-1}$ and $\sigma_a = \frac{1}{3}\left(2^{-5}\right) cm^{-1}$. We ran this problem on an orthogonal mesh using an S_8 Square Chebyshev quadrature set. Results of the convergence rate test problem are shown in Figure 2. The results show BLD, PWLD and PWBLD have extremely similar accuracy for this simple truncation error test problem.

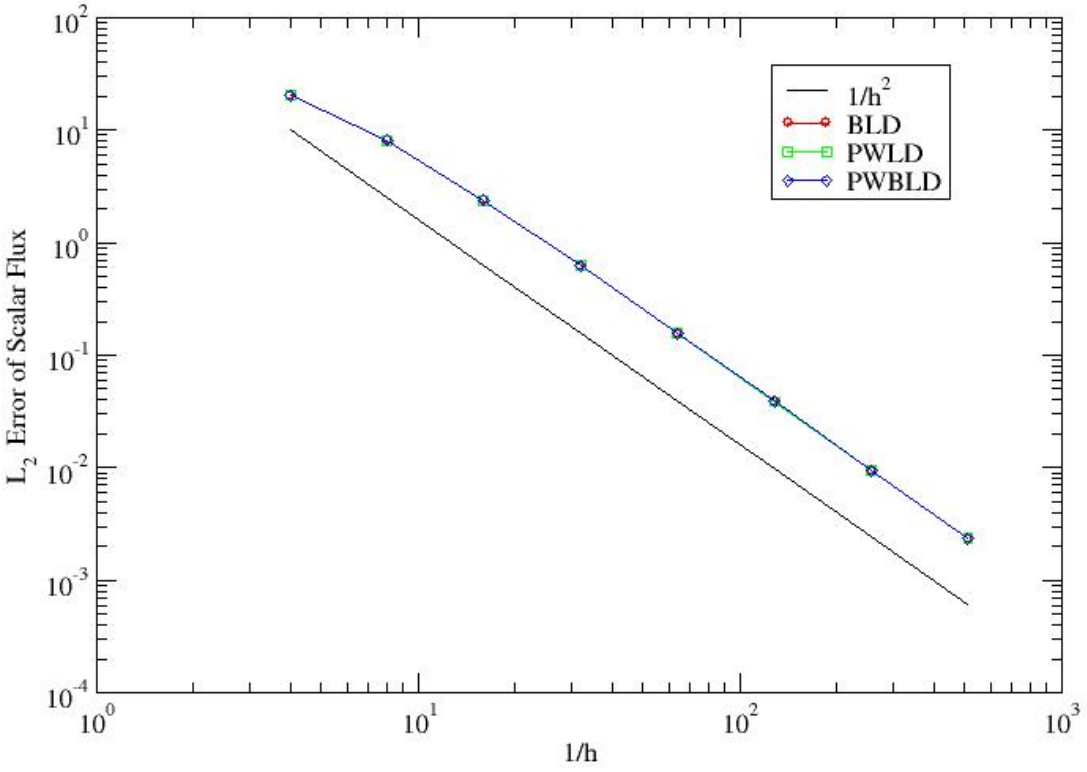

Figure 2: Truncation Error of multiple methods on a diffusive test problem

An important issue when considering the thick diffusion limit is related to the accuracy of the numerical solution on the interior of a thick and diffusive problem in the presence of unresolved boundary layers [12, 14]. The following numerical results are intended to illustrate that the PWLD and PWBLD methods produce reasonably accurate solutions on the problem interior, even though the boundary layers are unresolved, which is highly desirable property for a spatial discretization of the Sn transport equation.

We compute solutions on a regular mesh of polygons and on a randomized version of the initial regular mesh, as shown in Figs. 3 and 4. When the mesh is randomized, any non-convex elements are first converted into convex elements to avoid cycles in the Sn transport sweeps. A boundary layer in the solution is introduced by specifying a beam source of unit current on the bottom face directed along the quadrature direction that is closest to being normally incident. An S8 triangular Chebyshev-Legendre quadrature is used with the Gauss-Legendre points oriented along the Y-axis and reflection boundary conditions are imposed on the left and right faces of the problem with a vacuum boundary condition on the top face. The resulting solutions can then be compared against a 1D spatially-analytic Sn solution with S8 Gauss quadrature. The 0.1 cm x 0.1cm problem is divided into a grid that roughly comprises 32 x 32 mesh elements [6]. The problem is thick and diffusive with a total cross section of 10^4 cm^{-1} and an absorption cross section of 4/3 10^{-3} cm^{-1}.

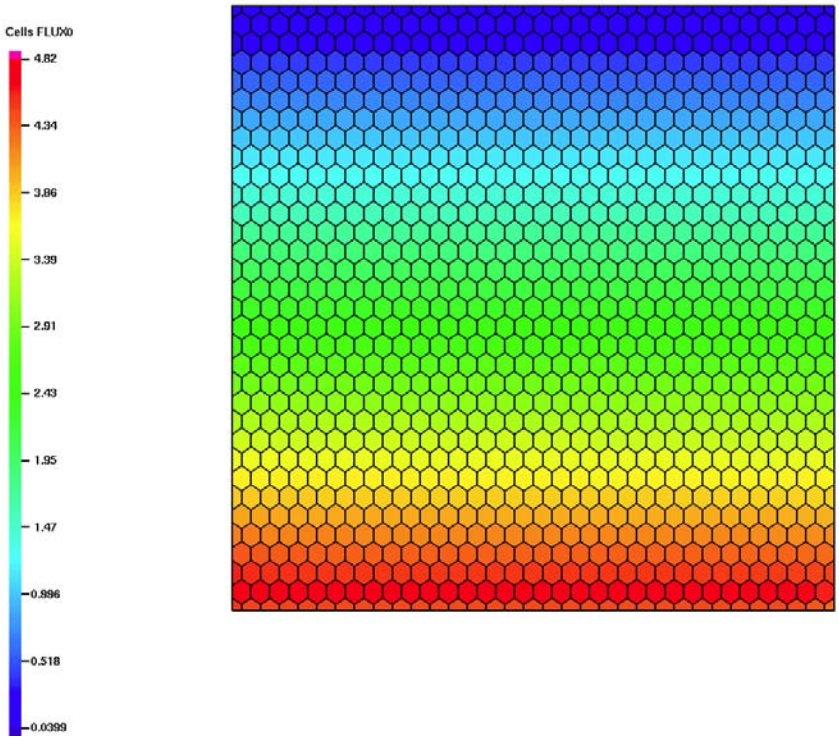

Figure 3: Regular Polygonal grid with the 1D diffusion problem solution

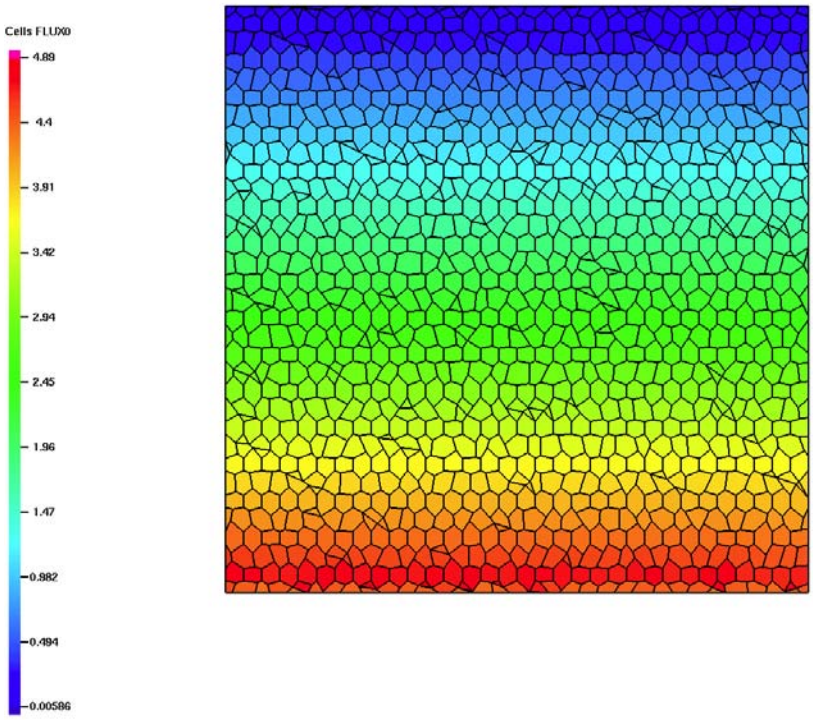

Figure 4: Randomized Polygonal grid with the 1D diffusion problem solution

Figures 5 and 6 show the computed cell-averaged scalar fluxes plotted at the y-coordinate of the centroid of each of the respective mesh cells. The PWLD and PWBLD method results are compared against the Continuous Finite Element-Based DFEM (CFEM-based DFEM) [6]. The CFEM-based DFEM is similar to the PWLD method in that it uses a triangular subdivision of the polygons to generate a local, linear CFEM spatial discretization over the triangles, but retains an extra degree of freedom at the polygon centroid (labeled “extra nodes” in the figures). Because any subdivision of the polygons can be used to develop the CFEM-based DFEM, the default implementation is to subdivide a polygon into well-shaped triangles that connect vertices of the polygon. However, it is not necessary to subdivide the polygon into triangles for the CFEM-based DFEM; it is also possible to subdivide into a mix of triangles and quadrilaterals and employ a mix of linear and bilinear discretizations to develop the local CFEM equations. For the CFEM-based DFEM results, we use a triangular LD discretization on mesh cells having three nodes, a quadrilateral BLD discretization on mesh cells having four nodes, and the CFEM-based DFEM discretization on cells with more than four nodes.

These numerical results show excellent agreement on the problem interior, even though the boundary is clearly not resolved by the mesh.

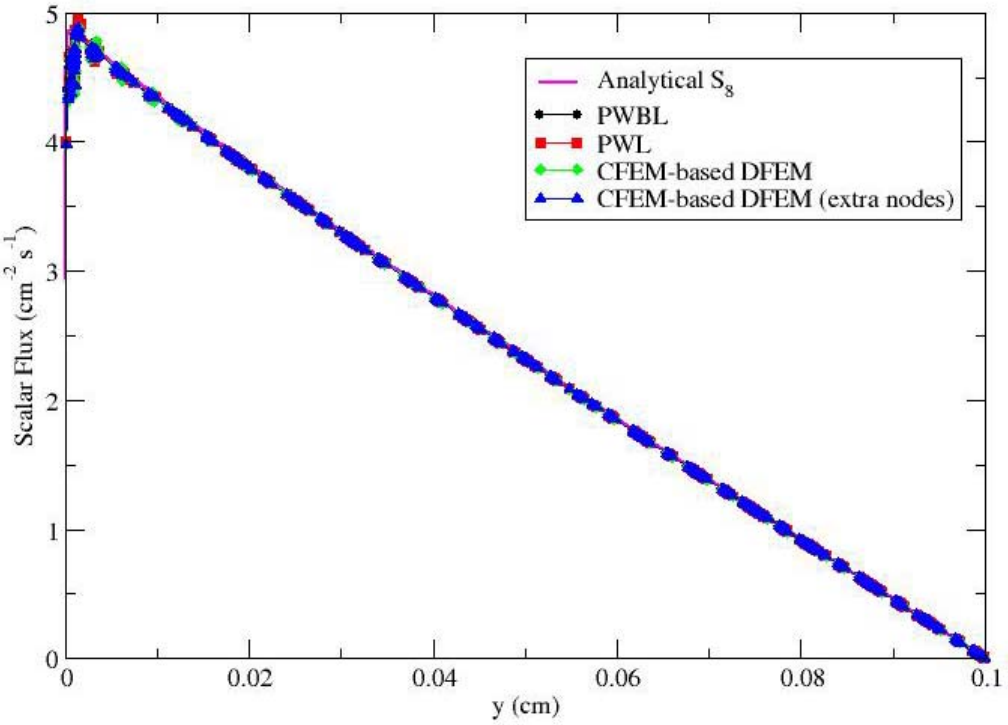

Figure 5: Scalar Fluxes on a Regular Polygonal grid for multiple discretizations

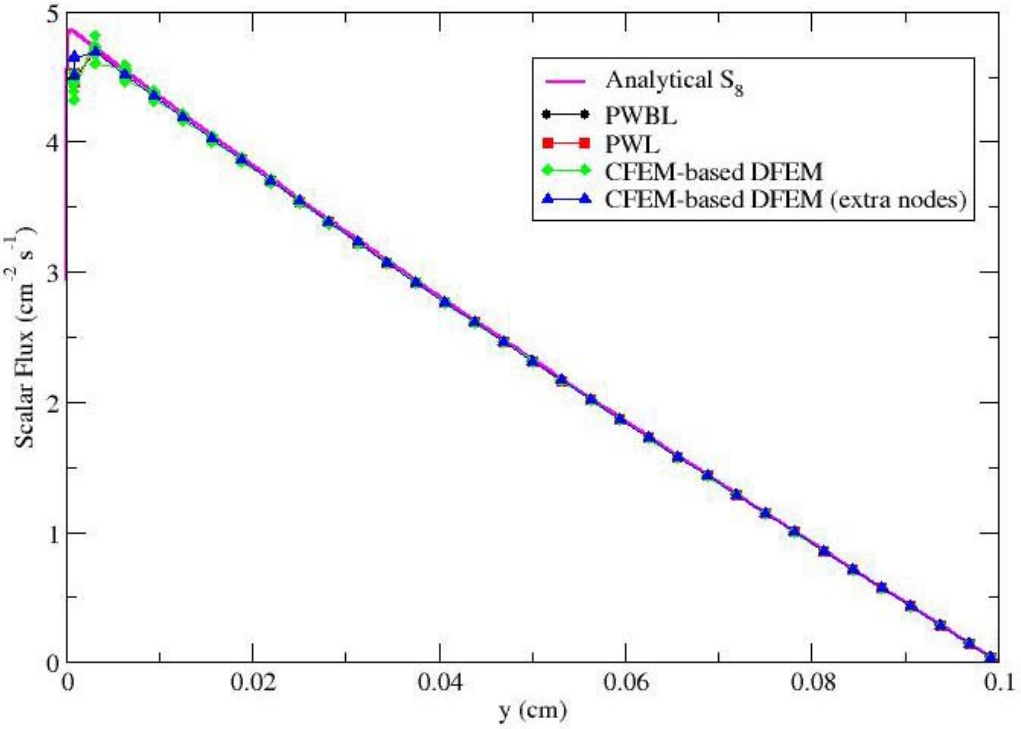

Figure 6: Scalar Fluxes on a Randomized Polygonal grid for multiple discretizations

6. CONCLUSION

The preliminary numerical results for the PWBLD method show great promise. The development of the method is similar to that of the PWLD method, but the basis functions are fundamentally different. These functions offer more curvature in the approximation, but their increased complexity will lead to increased computational cost. The amount of this increased computational cost has not yet been investigated. Because of the similarity to PWLD, we expect that PWBLD will perform as well as the previously developed methods for X-Y geometry. We have shown that PWBLD is equivalent to BLD on quadrilateral grids and behaves as well as PWLD on multiple numerical test problems in the diffusion limit.

In this paper we have presented only an introduction to the PWBLD method and the newly defined PWBL basis functions. Additional work is required to fully characterize the method. First, we would like to extend PWBLD to R-Z geometry. This is straightforward and should yield similar behavior to the X-Y results. Second, it is essential to complete the detailed asymptotic analysis to mathematically verify and support our assertion that the PWBLD method has the thick diffusion limit. The asymptotic analysis that was developed for general DFEMs [8] and for the PWLD method [1, 7, 10] can be adapted for the PWBLD method in both X-Y and R-Z on arbitrary polygonal grids.

Extending the PWBLD method to 3D polyhedral grids presents a challenging problem. We have not yet found a consistent way to subdivide the polyhedral cells into hexahedral subcell volumes. This 3D extension will be an important topic of future work because only 2 other spatial discretizations, PWLD and Upstream Corner Balance, have been shown to retain good numerical properties in the thick diffusion limit on 3D arbitrary polyhedral grids [3, 10], although the CFEM-based DFEM [6] can also be similarly extended to tetrahedral, hexahedral or other types of sub-elements.

ACKNOWLEDGMENTS

This work performed under the auspices of the U.S. Department of Energy by Lawrence Livermore National Laboratory under Contract DE-AC52-07NA27344. LLNL-CONF-464892

REFERENCES

1. H. G. Stone and M. L. Adams, “A Piecewise Linear Finite Element Basis with Application to Particle Transport,” *Proc. ANS Topical Meeting Nuclear Mathematical and Computational Sciences Meeting,* Gatlinburg, TN, April 6-11, 2003, CD-ROM (2003).
2. H. G. Stone and M.L. Adams, “New Spatial Discretization Methods for Transport on Unstructured Grids,” *Proc. ANS Topical Meeting Mathematics and Computation, Supercomputing, Reactor Physics and Biological Applications,* Avignon, France, September 12-15, 2005, CD-ROM (2005).
3. M. L. Adams, “Subcell Balance Methods for Radiative Transfer on Arbitrary Grids,” *Transport Theory Statist. Phys.* **26**, 385-431, (1997).

4. G. G. Davidson and T. S. Palmer, “Finite Element Transport Using Wachspress Rational Basis Functions on Quadrilaterals in Diffusive Regions,” *Nucl. Sci. and Eng.* **159**, 242-255 (2008).
5. E. Wachspress, “Generalized Finite Elements,” *Proc. International Conference on Mathematics and Computational Methods & Reactor Physics,* Saratoga Springs, New, NY, May 3-7, 2009, CD-ROM (2009).
6. J. S. Warsa, “A Continuous Finite Element-Based, Discontinuous Finite Element Method for S_N Transport,” *Nucl. Sci. and Eng.* **160**, 385-400 (2008).
7. T. S. Bailey, M. L. Adams, J. H. Chang, J. S. Warsa, “A Piecewise Linear Discontinuous Finite Element Spatial Discretization of the Transport Equation in 2D Cylindrical Geometry,” *Proc. International Conference on Mathematics and Computational Methods & Reactor Physics*, Saratoga Springs, New, NY, May 3-7, 2009, CD-ROM (2009).
8. M. L. Adams, “Discontinuous Finite Element Transport Solutions in Thick Diffusive Problems,” *Nucl. Sci. and Eng.* **137**, 298-333 (2001).
9. E. E. Lewis and W. F. Miller, *Computational Methods of Neutron Transport*, American Nuclear Society, La Grange Park, Il (1993).
10. T. S. Bailey, “The Piecewise Linear Discontinuous Finite Element Method Applied to the RZ and XYZ Transport Equations,” Doctoral Dissertation, Texas A&M University (2008).
11. T. A. Wareing, J. M. McGee, J. E. Morel, and S. D. Pautz, “Discontinuous Finite Element S_N Methods on Three-Dimensional Unstructured Grids,” *Nucl. Sci. and Eng.* **138**, 256-268 (2001).
12. J. E. Morel and J. S. Warsa, “Spatial Finite-Element Lumping Techniques for the Quadrilateral Mesh S_n Equations in X-Y Geometry,” *Nucl. Sci. and Eng.* **156**, 325-342 (2007).
13. J. E. Morel and J. S. Warsa, “A Lumped Bi-Linear Discontinuous S_n Spatial Discretization for RZ Quadrilateral Meshes,” *Trans. Am. Nucl. Soc.*, **95**, 873-875 (2006).
14. J. E. Morel and E. W. Larsen, “Asymptotic Solutions of Numerical Transport Problem in Optically Thick, Diffusive Regimes II, *Journal of Computational Physics*, **83**, 212-236 (1989).